HIDDEN MARKOV MODELS FOR TRACKING NEURONAL STRUCTURE CONTOURS IN ELECTRON MICROGRAPH STACKS

Min-Chi Shih, Kenneth Rose

Department of Electrical and Computer Engineering
University of California, Santa Barbara, CA 93106
{minchi_shih,rose}@ece.ucsb.edu

ABSTRACT

This paper is focused on the problem of tracking cell contours across an electron micrograph stack, so as to discern the 3D neuronal structures, with particular application to analysis of retinal images. While the problem bears similarity to traditional object tracking in video sequences, it poses additional significant challenges due to the coarse z-axis resolution which causes large contour deformations across frames, and involves major topological changes including contour splits and merges. The method proposed herein applies a deformable trellis, on which a hidden Markov model is defined, to track contour deformation. The first phase produces an estimated new contour and computes its probability given the model. The second phase detects low-confidence contour segments and tests the hypothesis that a topological change has occurred, by introducing corresponding *hypothetical arcs* and re-optimizing the contour. The most probable solution, including the topological hypothesis, is identified. Experimental results show, both quantitatively and qualitatively, that the proposed approach can effectively and efficiently track cell contours while accounting for splitting, merging, large contour displacements and deformations.

***Index Terms*—** Electron micrograph, neuronal structure tracking, hidden Markov model, topological change

1. INTRODUCTION

Recent advances in imaging have enabled visual inspection of image stacks at the scale of a few nanometers, which provides new paths to understanding of cellular ultrastructure. However, manual analysis is labor intensive and impractical for huge volumes of image data. Automatic high-throughput techniques are needed to acquire complete cell and network maps. In this paper we consider the problem of tracking contours of neuronal structures across z-slices in electron micrograph (EM) stacks. This problem is somewhat similar to object tracking in video sequences, where the main challenges involve translation, deformation, and changing of illumination or contrast [1]. However, the challenges here are exacerbated in several ways. The coarse z-direction resolution of EM images causes larger displacements and considerable non-rigid deformations. Moreover, the neuronal structures are complex and the contours undergo major topological changes, i.e., splitting and merging. At the extreme, experimental artifacts such as registration errors during the process of mosaicking lead to dramatic displacements.

This work was supported by the NSF under grant OIA 0941717. The authors thank Dr. Robert Marc, Dr. Bryan Jones and Dr. James Anderson from the Univ. of Utah for providing data used in experiments.

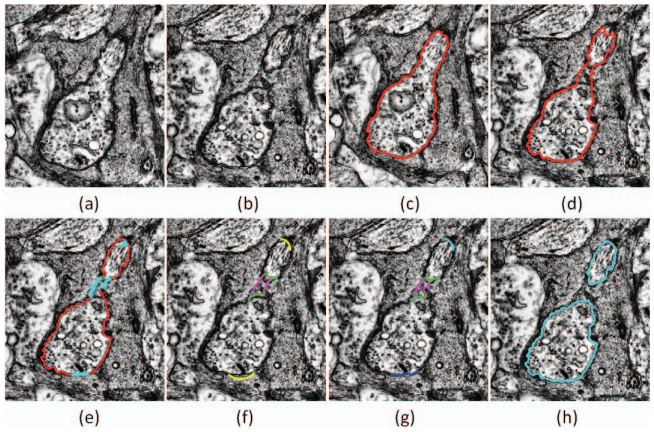
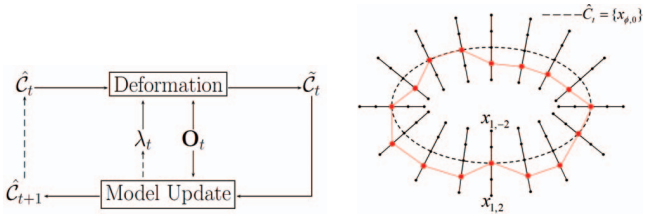


Fig. 1. (Best in color) (a), (b): an example of splitting in 2 consecutive frames; (c), (d): results of traditional HMM-based methods; (e): uncertain segments; (f): hypothetical arcs associated with the uncertain segments; (g): result contours after deforming the hypothetical arcs; (h): result of the proposed method, which successfully captures the splitting.

We employ the paradigm of a deformable trellis on which a hidden Markov model (HMM) is defined to track contours from frame to frame. A multi-cue HMM framework was proposed in [2] for face tracking. The probabilistic nature of HMM allows easy integration of multiple cues from observations, and enables computationally feasible global optimization via the efficient dynamic programming algorithm [3]. In [4], an enhanced HMM technique was proposed for tracking open-contour objects in biological image sequences, such as microtubules. More recently, [5] added a part-based representation to a generalized HMM framework for closed-contour face tracking and achieved higher accuracy. However, the existing HMM methods are insufficient to handle 3D neuronal structures mainly due to the problems of topological changes. They, in fact, underperform non-parametric methods such as level set methods [6], which naturally capture topological changes.

A relevant work of parametric tracking in electron micrograph can be found in [7], where Kalman-snakes and optical flows are used to track axons over hundreds of frames. However, the target objects do not split or merge, and the deformation and translation in their data set is relatively small. In [8], segmentation is performed on each frame to acquire all cells (or neurons), which are then matched over frames to achieve 3-D reconstruction. However, to the best of our knowledge, no single segmentation method works well on highly



(a) (b)

Fig. 2. (a)system block diagram, (b)an example of deformable trellis. The black dashed curve is the initial contour, and the red solid connected line is the estimated contour.

cluttered data as we have had to segment every cell. In [9], an active contour framework is proposed to tackle the sub-problem of splitting, but leaves the merging problem unsolved. In this paper, we propose a novel parametric HMM framework to handle the aforementioned challenges. It preserves the inherent precision advantage of HMM in terms of accurate contour location, and additionally handles the problem of topological changes.

2. DEFORMABLE TRELLIS AND HIDDEN MARKOV MODEL

The overall tracking procedure is depicted, at the high level, in Fig. 2(a), following the paradigm of [4]. Given frame t in the image sequence, together with the initial contour $\hat{C}_t$ of an object of interest, we deform $\hat{C}_t$ to the estimated contour $\tilde{C}_t$. The deformation accounts for the observation $\mathbf{O}_t$ in the current image and the current HMM parameters λ_t. The parameters λ_t are updated before reaching the next frame, and $\tilde{C}_t$ is used as the initial contour for frame $t+1$. To initiate the deformation, we construct a trellis about contour $\hat{C}_t$. The trellis nodes are points on each normal to the contour and represent the states of the hidden Markov model, and hence any path through the trellis is a potential new contour, as shown in Fig. 2(b).

The HMM is determined by $\lambda = (\pi, A, B)$, which consists of prior π, transition probabilities A, and observation probabilities B. The output $\mathbf{q}$ is a sequence of states, each of which is a position on a normal line in the trellis, and they jointly determine a contour. By letting q_ϕ be the ϕ-th state of the sequence, and $\mathbf{o}_\phi$ be the observation at time ϕ, we can define $\pi_\psi = P(q_1 = \psi)$, $a_{\psi',\psi} = P(q_\phi = \psi | q_{\phi-1} = \psi')$, and $b_{\phi,\psi} = P(\mathbf{o}_\phi | q_\phi = \psi)$, where $\psi \in \{-\Psi, \dots, 0, \dots, \Psi\}$, and $\phi \in \{1, 2, \dots, \Phi\}$. The goal now is to find the state sequence that best explains the observation. The most probable state sequence is $\mathbf{q}^* = \underset{\mathbf{q}}{\operatorname{argmax}} \left\{ \pi_{q_1} \prod_{\phi=2}^{\Phi} P(q_\phi | q_{\phi-1}) \prod_{\phi=1}^{\Phi} P(\mathbf{o}_\phi | q_\phi) \right\}$, and the exact solution can be found using the Viterbi algorithm at complexity $O\left(\Phi(2\Psi+1)^2\right)$. In addition, with the forward-backward algorithm we can compute the likelihood of each state, which provides a local measure of confidence.

A part-based representation for HMM was later proposed to cluster the entire contour into parts, and compute local parameters for each part according to its characteristics [5]. In this way we model the non-stationary nature of the contour statistics, as is often the case in practice. It has been demonstrated that the part-based representation is more robust than the globally homogeneous model.

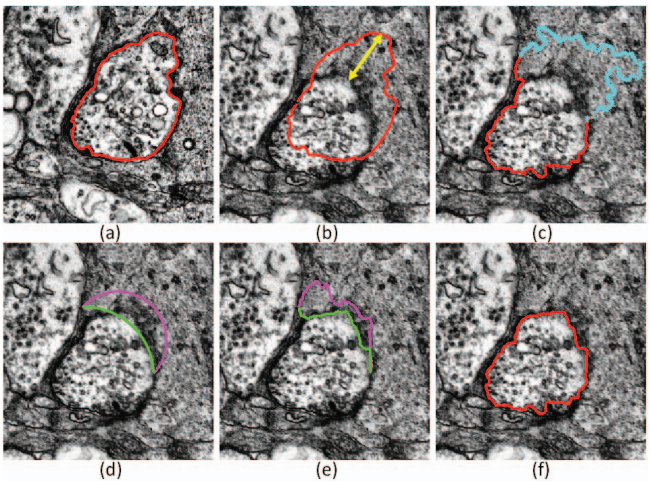


Fig. 3. (Best in color) (a), (b): an example of large displacement in 2 consecutive frames, where the translation exceeds 50 pixels (yellow arrow in (b)); (c): results of traditional HMM-based methods and the uncertain segments; (d): 2 hypothetical arcs are created associated with the uncertain segments; (e): result contour after deforming the hypothetical arcs; (f): result of the proposed method, which successfully captures the real contour.

3. PROPOSED METHOD

3.1. Features and Observation Probability

In the proposed scheme, the observation $\mathbf{o}_\phi(\psi)$ for one point $x_{\phi,\psi}$ in the trellis is measured via one region-based and two edge-based features. The region-based feature $\mathbf{o}_\phi^R(\psi)$ captures local characteristics inside the object contour near that point. The edge features $\mathbf{o}_\phi^{E1}(\psi)$ and $\mathbf{o}_\phi^{E2}(\psi)$ involve the 1^{st} and 2^{nd} order average gradients along the normal line. The observation probability is $b_{\phi,\psi} = f_\phi^R(\psi) f_\phi^{E1}(\psi) f_\phi^{E2}(\psi)$, where the features are assumed to be independent Gaussians.

3.2. Topological Changes and More

Here we define a segment $\tilde{C}_i = \{\tilde{C}_{i1}, \tilde{C}_{i2}, \dots\}$ on the contour $\tilde{C}_t = \{\tilde{C}_{t1}, \tilde{C}_{t2}, \dots\}$ to be *uncertain* if $L_{avg}(\tilde{C}_{ik}) < L_{avg}(\tilde{C}_{tk}) - \sigma_{\tilde{C}_{tk}}$, where $L_{avg}(\cdot)$ is the average observation probability at every point on the contour segment, i.e. a local measure of likelihood, and σ is the standard deviation. The segments with high confidence are left untouched, while we consider uncertain segments as candidates for topological changes.

For each uncertain segment $\tilde{C}_i$, we create one or more *hypothetical arcs* $\{H_{i1}, H_{i1}, \dots\}$ as new initial contours, and we deform all H_{ij}'s to obtain new estimated contours $\tilde{C}_{t,ij}$'s. The H_{ij}'s are fixed at the 2 end points of $\tilde{C}_i$, and they only differ in their curvatures. We compare all average likelihoods of the newly generated estimated contours $\tilde{C}_{t,ij}$'s and the original uncertain contour $\tilde{C}_i$, only the most likely contour survives. Therefore, the final contour maximizes the likelihood over all the choices considered. Please note that we average local likelihoods of all points on each contour, instead of the sum of likelihoods, hence eliminate dependence on contour length. In the following paragraphs, we explain how to use hypothetical arcs to aid HMM with the problem of topological changes.

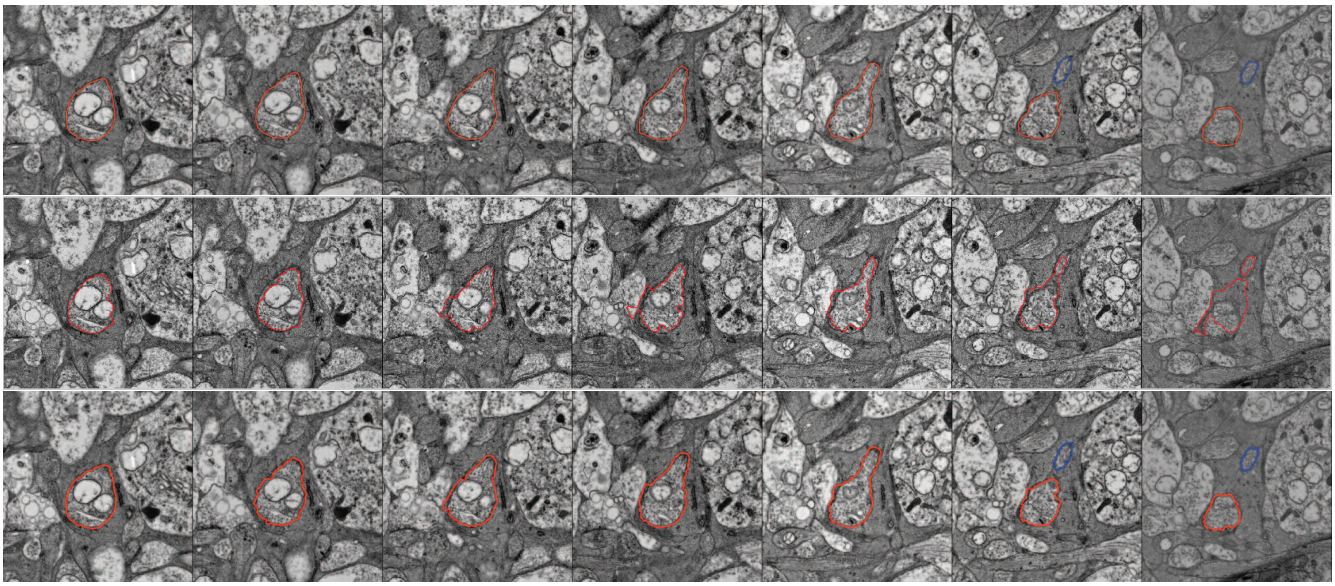


Fig. 4. (Best in color) The first row shows the ground truth of the objects of interest in seven frames(left to right). The second row shows the result of [6], and the third row shows the result of our proposed method.

3.2.1. Splitting Scenarios

When the object of interest splits into two, see Fig. 1 (a), (b), traditional HMM-based tracking algorithms tend to keep tracking the combined outer contour which covers both objects, see the red contours in Fig. 1 (c), (d). Since the parts of the contour between two objects are in fact not object boundaries, they are most likely to be detected as uncertain segments, see the cyan-colored segments in Fig. 1 (e). To detect a possible splitting situation, we define the following criteria:

1. there are two uncertain segments $\tilde{C}_p = \{\tilde{C}_{p1}, \tilde{C}_{p2}, \dots\}$ and $\tilde{C}_q = \{\tilde{C}_{q1}, \tilde{C}_{q2}, \dots\}$,
2. $\min_{i,j}\{d(\tilde{C}_{pi}, \tilde{C}_{qj})\} < \epsilon_{s1}$,
3. $\min_{i,j}\{g(\tilde{C}_{pi}, \tilde{C}_{qj})\} > \epsilon_{s2}$,

where $d(\cdot,\cdot)$ is the Euclidean distance of two points on the xy-plane, $g(\cdot)$ is the geodesic distance along the contour $\tilde{C}_t$, and ϵ's are fixed thresholds. The second criterion requires that the two uncertain segments be close in the xy-plane to support a possible split. The third criterion avoids false alarms when two uncertain segments are virtually contiguous.

Once the criteria are satisfied, the "split hypothesis" is activated, and we test it as follows. We create two pairs of hypothetical arcs, e.g. the magenta-colored and green-colored arcs in Fig. 1 (f), representing the hypothesis is "true" and "false" respectively (where the yellow arcs are not associated with splitting). We deform all the hypothetical arcs and obtain their corresponding estimated contours, see Fig. 1 (g). By choosing the pair of output estimated contours with higher likelihood, we decide whether the splitting hypothesis is more likely.

3.2.2. Merging Scenario

When dealing with merging scenarios, we first apply traditional HMM-based tracking process for multiple objects, and then detect whether a merging exists with the following criteria:

1. there are two objects with contours $\tilde{C}_k$ and $\tilde{C}_l$,
2. $\min_{i,j}\{d(\tilde{C}_{ki}, \tilde{C}_{lj})\} < \epsilon_{m1}$,
3. $\mathfrak{D}(\tilde{C}_k, \tilde{C}_l) < \epsilon_{m2}$,

where $\mathfrak{D}(\cdot,\cdot)$ is the Kullback-Leibler(KL) divergence of the pixel-intensity distributions inside the two object contours. KL divergence measures the difference of two probability distributions. We use the symmetric KL version: $\mathfrak{D}(\mathbf{d_1}, \mathbf{d_2}) = \widetilde{\mathfrak{D}}(\mathbf{d_1}, \mathbf{d_2}) + \widetilde{\mathfrak{D}}(\mathbf{d_2}, \mathbf{d_1})$, where $\mathfrak{D}$ is the standard asymmetric KL divergence. The criteria ensure that we only merge two nearby objects with similar internal characteristics. Once the criteria are satisfied, we activate the " merge hypothesis" and test it similarly to the splitting scenario. We compare the likelihood of the two pairs of the deformed hypothetical arcs and decide whether the hypothesis is validated.

3.2.3. Large Displacement Scenario

Hypothetical arcs can help not only in the splitting and merging scenario, but also when there is large displacement of an object within two consecutive frames. In large scale and high-definition biological images sequences, an object can suddenly shift by more than fifty pixels away, and existing HMM-based algorithms would lose its track. In this case we can also create hypothetical arcs for the uncertain segments, and find the optimal estimation for the object contour. An example is shown in Fig. 3, where there is an obvious registration error in the second frame, which results in sudden large displacement. The true contour can be found by deforming the hypothetical arcs with similar procedures described in section 3.2.1 and 3.2.2.

4. EXPERIMENTAL RESULT

In the experiments we consider tracking contours of neuronal structures in electron micrograph stacks. First, we apply the proposed algorithm on 15 neuron structures without splitting and merging. The

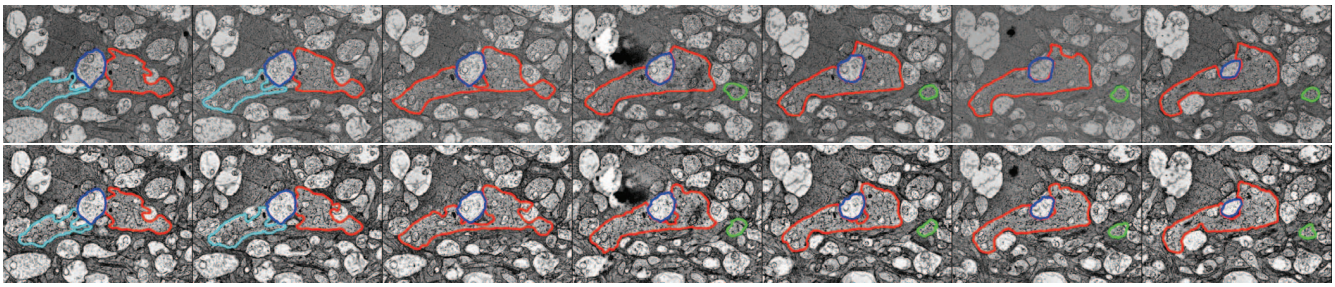


Fig. 5. (Best in color) An example of both splitting and merging. The first row shows the ground truth of the objects of interest in 6 frames(left to right). The second row shows the tracking result from the proposed method.

Table 1. Comparison of our proposed method and Chan-Vese method on EM image sequences.

	Chan-Vese method	Proposed method
F-measure	0.8079 ± 0.1262	0.9217 ± 0.0587
MAD	8.8354 ± 5.0559	1.9474 ± 0.7465
HD	34.4051 ± 26.7430	9.1608 ± 5.1571

experiments are performed for over 20 z-slices of the EM stack. Second, we use the proposed algorithm to track the contour of a single neuronal structure which splits into two in 7 z-slices, see Fig. 4. Finally, we apply the proposed algorithm on multiple neuronal structures which split and merge within 7 z-slices, see Fig. 5.

Our results are compared with the classic Chan-Vese level set method with the implementation of [10]. To measure the performance, we use three different error metrics, a) F-measure, b) mean-absolute-distance (MAD), and c) Hausdorff distance (HD). F-measure is region-based score to be maximized, while MAD and HD measures are distance-based costs to be minimized. Let $C_g = \{c_{g1}, c_{g2}, \ldots, c_{gm}\}$ be the manually annotated ground truth of the object contour, and $C_r = \{c_{r1}, c_{r2}, \ldots, c_{rn}\}$ be the resulting object contour from an automatic algorithm. MAD and HD are defined as follows:

$$\text{MAD}(C_g, C_r) = \frac{1}{2}\left(\frac{1}{m}\sum_{i=1}^{m} d_m(c_{gi}, C_r) + \frac{1}{n}\sum_{i=1}^{n} d_m(c_{ri}, C_g)\right)$$

$$\text{HD}(C_g, C_r) = \max\left(\max_i d_m(c_{gi}, C_r), \max_i d_m(c_{ri}, C_g)\right),$$

where $d_m(c_{gi}, C_r) = \min_j |c_{gi} - c_{rj}|$. Given the available ground truth, preliminary results show that our proposed algorithm outperforms the Chan-Vese method, (see Table 1). We note that there exist many variants of the level sets algorithm, and we choose to compare with the classic Chan-Vese method. The proposed algorithm is coded in MATLAB, and, despite no further code optimization, the computation time is less than 1 sec per object per frame.

5. CONCLUSION

This paper presents a novel topology-aware hidden Markov model-based contour tracking algorithm for tracking contours of neuronal structures in an electron micrograph stack. An estimated contour is produced together with the confidence of each point on it computed according to the HMM. We detect segments of low confidence and use hypothetical arcs to test hypotheses of topological changes, such as splitting and merging, and then identify the most probable solution. Experimental results show, both qualitatively and quantitatively, the capability of tracking contours of neuronal structures which split, merge, and deform, with the existence of cluttered backgrounds. This provides an alternative parametric solution for the problems of topological changes.

6. REFERENCES

[1] A. Yilmaz, O. Javed, and M. Shah, "Object tracking: A survey," *ACM Comput. Surv.*, vol. 38, no. 4, 2006.

[2] Y. Chen, Y. Rui, and T. S. Huang, "Multicue HMM-UKF for real-time contour tracking," *IEEE Trans. Pattern Anal. Mach. Intell.*, vol. 28, no. 9, pp. 1525–1529, 2006.

[3] L. Rabiner, "A tutorial on hidden Markov models and selected applications in speech recognition," *Proc. IEEE*, vol. 77, no. 2, pp. 257–286, 1989.

[4] M.E. Sargin, A. Altinok, B.S. Manjunath, and K. Rose, "Variable length open contour tracking using a deformable trellis," *Image Processing, IEEE Transactions on*, vol. 20, no. 4, pp. 1023 –1035, april 2011.

[5] M.E. Sargin, *Probabilistic graphical models for motion analysis and object tracking*, Ph.D. thesis, UC Santa Barbara, 2010.

[6] T.F. Chan and L.A. Vese, "Active contours without edges," *Image Processing, IEEE Transactions on*, vol. 10, no. 2, pp. 266 –277, feb 2001.

[7] E. Jurrus, T. Tasdizen, P. Koshevoy, P.T. Fletcher, M. Hardy, C.B. Chien, W. Denk, and R. Whitaker, "Axon tracking in serial block-face scanning electron microscopy," in *In Workshop on Microsc. Image Anal. with Appl. in Biol*, 2006.

[8] E. Jurrus, R. Whitaker, B.W. Jones, R. Marc, and T. Tasdizen, "An optimal-path approach for neural circuit reconstruction," in *Biomedical Imaging: From Nano to Macro, 2008. ISBI 2008. 5th IEEE International Symposium on*, may 2008, pp. 1609 –1612.

[9] C. Zimmer, E. Labruyere, V. Meas-Yedid, N. Guillen, and J.-C. Olivo-Marin, "Segmentation and tracking of migrating cells in videomicroscopy with parametric active contours: a tool for cell-based drug testing," *Medical Imaging, IEEE Transactions on*, vol. 21, no. 10, pp. 1212 –1221, oct. 2002.

[10] S. Lankton, "Level set method implementation. http://www.shawnlankton.com/tag/level-sets/," .